Physics AUC, vol. 30 (part I), 56-60 (2020) **PHYSICS AUC**

Effect of Ni-doping on the Defect Densities Associated with Photoluminescence from ZnO Quantum Dots

PIJUS KANTI SAMANTA
Department of Physics (PG & UG), Prabhat Kumar College, Contai-721404, West Bengal, India
E-mail: pks.pkcphy@gmail.com

Abstract

A simple wet chemical method has been reported here to prepare pure and nickel doped zinc oxide quantum dots. Room temperature photoluminescence spectroscopy was deployed to investigate the optical emission properties of the synthesized materials. Both undoped ZnO and Ni/ZnO show sharp and strong PL emission at 691 nm along with very low intense UV emission at 392 nm. The PL emission peak at 392 nm is assigned for direct band edge transition in ZnO. The PL emission peak at 691 nm is attributed to specific defect states in ZnO. A detail investigation of the defect states revealed that the PL emission peak at 691 may arise due to trapped holes of V_O^{++} states and CB edge. We also discussed the mechanism of Ni-doping in ZnO crystal.

Keywords: ZnO, Doping, Photoluminescence, Quantum-confinement, Defect-density.

1. INTRODUCTION

Nanomaterials are in the forefront of research due to their unique enhanced properties as compared to their bulk counterpart [1]. In nanocrystals, the carriers are confined in a very small region leading to discrete energy spectrum. The quantum dots (QDs) are very small particles of materials where the motion of the carriers is quantized in all the three dimensions. In these QDs, confinement of carriers may be strong or weak depending on the size of QDs. The critical size in these cases is determined with reference to the Bohr radius. The density of states D(E) of QDs is discrete leading to unique optical and electronic properties [2,3]. Zinc oxide (ZnO) is a II-VI semiconductor and very well known for its optical emissions. It has a very high band gap of 3.37 eV and large excitonic binding energy of 60 meV at room temperature [4]. This makes it a potential material for UV-laser. It usually exhibits photoluminescence in the UV region due to band edge transition. However, in chemical growth of ZnO crystals at low temperature, several defect states (oxygen and zinc vacancy, interstitial states) are created [5, 6]. These defect states have energy in between the valence band and conduction band of ZnO. Hence any transition occurring between these defect states gives rise to photo-luminescence in the visible region of wavelength. These defect states may also be created due to doping of foreign atom in ZnO [7]. If the densities of these defect states are very large then the band edge emission may be suppressed by the defects associated emission. Hence the only photoluminescence will be the defect mediated visible photoluminescence.

Chemical method is a very popular technique to synthesize ZnO quantum dots of high yield.

By varying the process conditions, the size of the QDs can be tuned very easily. Green and non-aquash synthesis of colloidal ZnO QDs of size ~ 8.3 nm is reported by Casa et. al.[8]. Mn-doped well crystalline ZnO QDs synthesis is also reported by Norberg et. al. by a hydrolysis and condensation reaction in DMSO under atmospheric conditions [9].

Here, in this paper, a simple synthesis method of growing pure and Ni-doped ZnO quantum dots has been reported. The photoluminescence from the synthesized materials was investigated further with a view to understand the effect of Ni-doping on the optical properties of ZnO. In this context the mechanism of incorporation of Ni atom in ZnO QDs is also discussed.

2. MATERIALS AND METHOD

2.1. Synthesis of pure ZnO QDs

Preparation of ZnO QDs by chemical method is very simple and cost effective and is reported elsewhere in [3, 4, 7]. All chemicals used in the synthesis of ZnO and Ni-doped ZnO (Ni/ZnO) were of analytical grade, sup-plied by Merck (99.99% pure) and used without further purification. We used methyl alcohol for preparing the solution of precursors. For the synthesis of pure ZnO, 0.49 g of zinc acetate dihydrate was added with 21 ml methanol to prepare 0.1 M solution. 0.15 g of NaOH was dissolved methyl alcohol to prepare 0.3 M solution. The zinc acetate solution was put under vigorous stir-ring. Under constant stirring for 1 hr, NaOH solution was added drop wise to maintain the pH of the solution above 11. The stirring was then further continued for 2 hr under a constant temperature of 60°C. At the end of the reaction a white precipitate was deposited at the bottom of the flask. The deposit was filtered, washed methyl alcohol and dried in a furnace at 100 ˚C further characterization.

2.2. Synthesis of Ni/ ZnO QDs

To synthesize Ni/ZnO, we followed the same experimental process as described in the previous section. We additionally used nickel acetate solution of predetermined concentration.

2.3. Material Characterization

Room temperature photoluminescence (PL) spectra were recorded in a Perkin Elmer LS-55 spectrophotometer to study the emission behaviour of undoped ZnO and Ni/ZnO QDs.

3. RESULTS AND DISCUSSIONS

Typical PL spectrum of undoped ZnO and Ni/ZnO in the wavelength range 350-750 nm is shown in Fig-1 and Fig-2. The both undoped ZnO and Ni/ZnO exhibit strong PL peak at 691 nm associated with a small UV peak at 392 nm. The PL emission peak at 392 nm is attributed to band edge emission of ZnO. To understand the emission peak at 691 nm we have to investigate the defect energetic of ZnO.

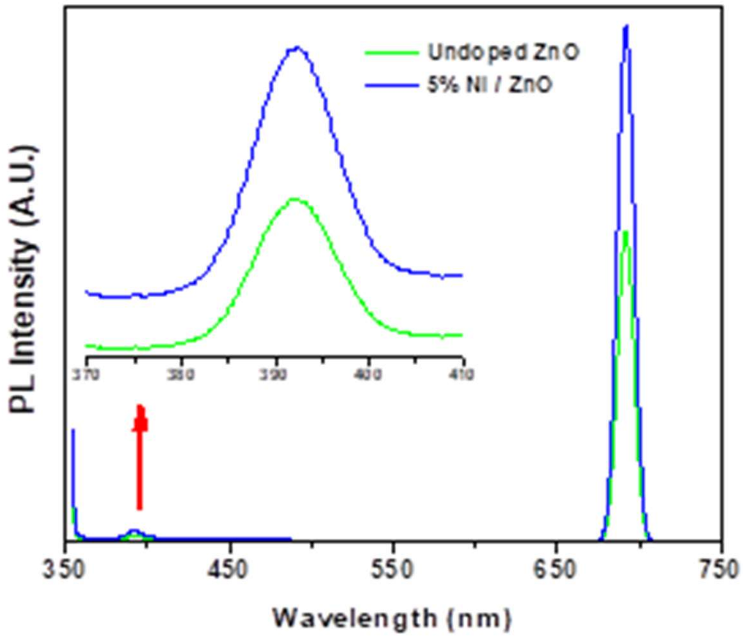

Fig. 1- Room temperature PL spectrum of undoped ZnO and Ni/ZnO QDs. Inset shows the enlarged view of UV peak.

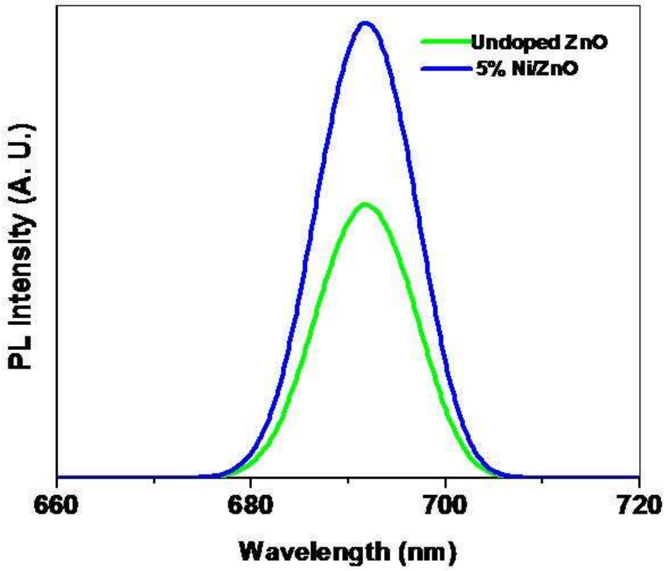

Fig. 2- PL spectra of undoped ZnO and Ni/ZnO.

Several researchers have calculated the defect energetic of ZnO using Full-Potential-Linear Muffin-Tin orbital method. The Full potential linear Muffin-Tin orbital model is based on density functional theory considering local density approximation. However, no approximation is made on the shape of the nanocrystals. For mathematical simplicity the muffin-tin sphere is divided into a number of tiny zones within which the Schrödinger's equation is solved. There is a recent re-port on the red emission from ZnO/PMMA nanocomposites by Mai et. al.[10]. The visible emission from ZnO is mainly due to several defect states like interstitial zinc (I_{Zn}), zinc vacancy (V_{Zn}), oxygen vacancy (V_O) and their inter-complexes. The energy state of I_{Zn} lies near the conduction band (CB) minima and produces two charged states I^{+}_{Zn} and I^{++}_{Zn}. Due to high formation energy, the concentration of V_O and I_{Zn} in ZnO is usually very small. But the I_{Zn}-V_O hybrid states are created due to Coulombic attraction between them which reduces the enthalpy of the combined state. This leads to hybrid $(I_{Zn})^*$ and $(V_{Zn})^*$ state [11-14]. The energy of this new state depends on the mutual separation between them. The (IZn)* state gives rise to UV-blue photoluminescence under the excitation of energy just below the band gap energy as reported in [10]. It is also reported that the energy states associated with I_{Zn}, $(I_{Zn})^*$ and V_O^{++} lie in the vicinity of CB minimum by a 0.1-0.6 eV and 2.0 eV respectively while the V_O^{+} state have energy 2.4 eV above the valence band (VB) maxima. Various energy states are shown in Fig. 3. The PL emission peak at 691 can be attributed to the trapped holes of V_O^{++} states and CB edge.

Table 1- Integrated intensities of different PL emission peak.

Peak position (nm)	**Integrated intensity (A.U.)**		**FWHM (nm)**	
	Undoped ZnO	Ni/ZnO	Undoped ZnO	Ni/ZnO
691	742.72	1235.97	11.87	11.86
392	8.80	15.02	9.98	10.12

The integrated intensities of the two emission peaks are also shown in table-1. We see that the integrated intensity of 691 nm peak for undoped ZnO is 742 while that for Ni/ZnO is 1235. This indicates that the doping of Ni in ZnO increases V_O^{++} states in ZnO. It is also observed that the UV emission due to Ni doping is also increased by the same ratio (see inset of Fig-1). This indicates the incorporation of Ni in ZnO increases the holes trapped in V_O^{++} states there by the intensity of the 691 peak for Ni/ZnO QDs enhances.

To understand the doping mechanism of Ni doping in ZnO first we look at the crystal structure of ZnO. ZnO crystallizes in wurtzite form in which Zn^{2+} and O^{2-} ions are stacked alternatively along the c-axis of the wurtzite lattice. The bottom face is O^{2-} ion terminated while the top face is terminated by Zn^{2+} ion. So, wurtzite ZnO possesses dipole moment directed along c-axis. The top and the bottom faces are polar while the other six faces are non-polar. During chemical growth, some of the Zn^{2+} ion of the top face is replaced by Ni^{2+} ion. The Ni^{2+} ion incorporation in ZnO crystal is shown schematically in Fig. 4.

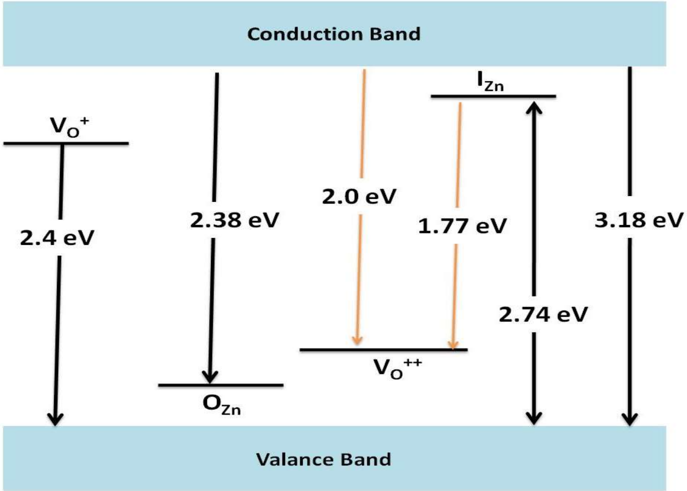

Fig. 3- Defect energy levels of ZnO.

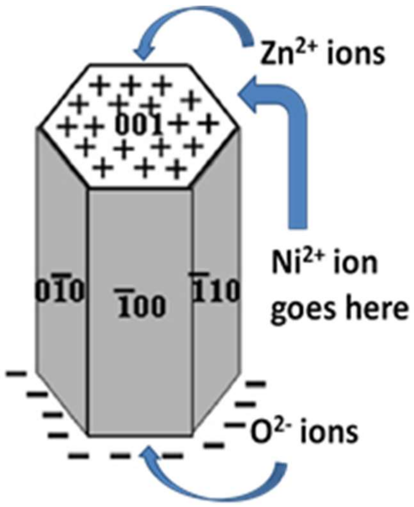

Fig. 4- Schematic of the Ni doping in ZnO crystal.

4. CONCLUSIONS

In conclusion, we have successfully synthesized un-doped and Ni doped ZnO QDs following sol-gel method. The undoped and doped ZnO QDs exhibit weak UV emission followed by strong red emission. The red PL emission peak at 691 was attributed to the trapped holes of V_O^{++} states and CB edge. Doping of Ni in ZnO enhances the intensity of the red emission and UV emission as well. However, this needs further investigations.

References

[1] J. Ma, F. Ji, D. Zhang, H. Ma, and S. Li, Thin Solid Films 357, 98 (1999).

[2] M. H. Huang, S. Mao, H. Feick, H. Yan, Y. Wu, H. Kind, E. Weber, R. Russo, and P. Yang, Science 292, 1897 (2001)

[3] D. P. Singh, Sci. Adv. Mater. 2, 245 (2010).

[4] D. Bera, L. Qian, S. Sabui, S. Santra, P. H. Holloway, Opt. Mater. 30, 1233 (2008).

[5] P. K. Samanta, J. Tissue Sci. Eng. 8, 2 (2017).

[6] S. I. Senatova, A. R. Mandal, F. S. Senatov, N. Y. Ani-simova, S. E. Kondakov, P. K. Samanta, D. V. Kuz-netsov, Current Nanoscience, 11(3), 354 (2015).

[7] V. Ponnarasan, Adv. Studies Theor. Phys., 8(6), 251 (2014).

[8] M. Casa, M. Sarno, L. Paciello, M. R. Beaumont, P. Ciambelli, Chemical Engineering Transactions, 47, 7 (2016).

[9] S. Nick, K. R. Norberg, E. J. Amonette, R. K. Kukka-dapu, D. A. Schwartz, D. R. Gamelin, J. Am. Chem. Soc. 126 (30), 9387 (2004).

[10] V. Mai, Q. Hoang, X. Mai, Adv. Mater. Sci. Eng., doi.org/10.1155/2018/7252809 (2018).

[11] K. Vanheusden, W. L. Warren, C. H. Seager et al., J. App. Phys., 79(10), 7983 (1996).

[12] Y. Kim, C. H. Park, Phy. Rev. Lett., 102(8), 086403 (2009).

[13] S. Hariharan, B. Karthikeyan, 183,1 (2017).

[14] Y. Kim and C. H. Park, Phy. Rev. Lett., 102(8), 086403 (2009).